CrystEngComm

Accepted Manuscript

ROYAL SOCIETY OF CHEMISTRY

www.rsc.org/crystengcomm

Journal Name

ARTICLE

A self-catenated *rob*-type porous coordination polymer constructed from triazolate and carboxylate ligands: fluorescent response to the reversible phase transformation

Received 00th January 20xx,
Accepted 00th January 20xx

DOI: 10.1039/x0xx00000x

www.rsc.org/

Mingli Deng,[a] Shijun Tai,[b] Weiquan Zhang,[a] Yongchen Wang,[a] Jiaxing Zhu,[a] Jinsheng Zhang,[b] Yun Ling*,[a] and Yaming Zhou [a]

A flexible structure of $\{[Zn_2(dmtrz)_2(L1)]\cdot 6H_2O\}_n$ (MAC-11) (Hdmtrz = 3,5-dimethyl-1H,1,2,4-triazole, H_2L1 = (E)-4,4'-stilbenedicarboxylic acid), which is a self-catenated *rob*-type net built of two-dimensional [Zn(dmtrz)] layers pillared by L1 ligands, has been solvothermally synthesized. It shows interesting thermo/water-induced reversible phase transformation accompanied by a photoluminescent response from 418 nm to 453 nm. Based on an iso-framework of $\{[Zn_2(dmtrz)_2(L2)]\cdot 4H_2O\}_n$ (MAC-13, H_2L2 = (E)-azobenzene-4,4'-dicarboxylic acid), a *pcu*-type framework of $\{[Zn_2(trz)_2(L1)]\cdot 4H_2O\}_n$ (MAC-14, Htrz = 1H, 1,2,4-triazole), a layer structure of [Zn(dmtrz)(HCOO)], a possible mechanism of the photoluminescent response to the reversible phase transformation for MAC-11 was also proposed.

Introduction

Flexible coordination polymers are of great interesting crystalline materials, especially those showing external stimuli-induced reversible structural changes accompanied by photoluminescent responses.[1-6] The intrinsic structural flexibility make them more promising in molecular recognition and sensing.[7-9] For examples, adsorption of CO_2 can be converted into detectable photoluminescent signals by incorporation of a fluorescent reporter distyrylbenzene (DSB) into a flexible structure of $Zn_2(bdc)_2(dabco)$;[10] aromatics can be well decoded by an interpenetrated dynamic frameworks because of distinct photoluminescent responses;[11] even high efficient sensing O_2 can be directly achieved by a flexible $[Cu(tez)]_n$.[12]

Up to now, several types of structures showing framework flexibility has been studied,[13-19] in which most of them are exclusively connected *via* metal-carboxylate coordination bonds. However, it has been argued due to its easy cleavage by H_2O.[20] Furthermore, even if these flexible frameworks are strong enough, there is still one challenge that is the distinguishable photoluminescent response to a phase transformation.[21, 22] Generally, most of the phase transformation of MOFs are caused by the adjustment of metal-carboxylate coordination angles.[23] This change could not lead to a sufficient change of energy state because coordinated carboxylate groups are separated with organic emitters by σ bonds (Scheme 1a).

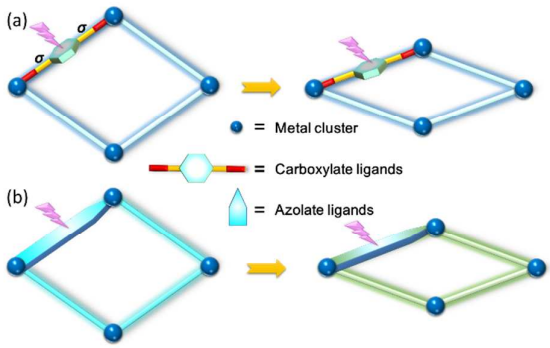

Scheme 1. A view of photoluminescent response to the framework flexibility, (a) the photoluminescent emission could not couple well with the framework change since the presence of σ (C-C) bonds; (b) in metal-azolates, the sensitivity of energy state to the structural change might be enhanced owing to the π-conjugated azolates are directly coordinated to metal ions.

Polyazoheterocycles, such as pyrazoles, imidazoles, triazoles, and tetrazoles, are promising ligands to construct robust coordination polymers because of the strong metal-nitrogen coordination bonds.[24-26] Taking the Zn_4O-based MOFs for an example, when the extendable group changes from carboxylate to azolate ligands, the framework stability in air and moisture condition can be greatly improved,[27,28] even the defect chemistry of the framework can be well-investigated in water.[27] Furthermore, azolate ligands can serve as an efficient superaexchange pathway and/or capacity for spin electrons, because the π-conjugated azolates are directly coordinated to metal ions. This characteristic has no doubt endue the energy

[a] *Shanghai Key Laboratory of Molecular Catalysis and Innovative Materials, Department of Chemistry, Fudan University, Shanghai, 200433, China.*
[b] *College of Chemistry, Chemical Engineering and Environmental Engineering, Liaoning Shihua University, Liaoning, 113001, China.*
* Corresponding author: yunling@fudan.edu.cn (Prof.Dr. Ling, Y.).
Electronic Supplementary Information (ESI) available: CIF data, Figures of PXRD, TGA, N_2 sorption etc. See DOI: 10.1039/x0xx00000x

state of metal-azolates more sensitive to the external stimuli-induced structural changes (Scheme 1b).

Recently, we have reported a series of porous coordination polymers constructed from triazolate and carboxylate ligands.[30-32] Encouraged by our previous works and taking the above mentioned issues in consideration, we propose to construct flexible porous structures in which the structural flexibility are originated from metal-azolates. In this paper, by combining photoluminescent 2D metal-triazolate with photoluminescnet stilbenedicarboxylic acid, a flexible and robust structure of $\{[Zn_2(dmtrz)_2(L1)]\cdot 6H_2O\}_n$ (MAC-11) (Hdmtrz = 3,5-dimethyl-1H,1,2,4-triazole, H_2L1 = (E)-4,4'-stilbenedicarboxylic acid) has been successfully isolated, which is a self-catenated *rob*-type net built of 2D [Zn(dmtrz)] layers pillared by L1 ligands. It can retain its framework integrity in water, and shows thermo/water induced reversible phase transformation accompanied by photoluminescent response from purple to blue. Furthermore, based on the isostructure of $\{[Zn_2(dmtrz)_2(L2)]\cdot 4H_2O\}_n$ (MAC-13, H_2L2 = (E)-azobenzene-4,4'-dicarboxylic acid), a *pcu*-type framework of $\{[Zn_2(trz)_2(L1)]\cdot 4H_2O\}_n$ (MAC-14, Htrz = 1H, 1,2,4-triazole), a layer structure of [Zn(dmtrz)(HCOO)] and the H_2L1 ligand, the possible mechanism of photoluminescent response to the reversible phase transformation was proposed for MAC-11.

Experimental

Materials and General characterization

All of the chemicals were obtained from commercial sources and were used without further purification, except Hdmtrz, H_2L2 ligands, which were synthesized according to previous literatures.[33-34] FT-IR spectra were recorded on a Nicolet 470 FT-IR spectrometer in the range of 4000–400 cm^{-1} on KBr pellets. Powder X-ray diffraction (PXRD) patterns were measured on a Bruker D8 powder diffractometer with Cu Kα radiation (λ = 1.5406 Å). Thermogravimetric analyses (TGA) were carried out on a TGA/SDTA 851 in the temperature range of 30–800 °C under N_2 flow with a heating rate of 10 °C ·min^{-1}. Elemental analyses of C, H, N were carried out on a Elementar Vario EL III. N_2 sorption at 77 K was measured on an ASAP 2020 gas adsorption apparatus (Micromeritics). Before gas adsorption, as-made sample (about 100 mg) was activated in methanol solution for 2 h and then degassed at 50 °C for 8 h. Photoluminescent measurements were performed on a Hitachi F-4500 fluorescence spectrophotometer equipped with monochromator (resolution: 0.2 nm) and 150 W Xe lamp.

Crystal Data Collection and Refinement

Data collection for MAC-11, MAC-13 and MAC-14 was carried out on a Bruker Apex Duo diffractometer with graphite monochromated Mo Kα radiation (λ= 0.71073 Å) at 293(2) K, respectively. Data reduction was performed with SAINT, and empirical absorption corrections were applied by SADABS program. Structures were solved by direct method using SHELXS program and refined with SHELXL program.[35-36] Heavy atoms and other non-hydrogen atoms were directly obtained from difference Fourier map. Final refinements were performed by full-matrix least-squares methods with anisotropic thermal parameters for all non-hydrogen atoms on F^2. C-bonded H atoms were placed geometrically and refined as riding modes. H atoms of lattice water were positioned from difference Fourier maps and then refined with rigid mode. Crystallographic data are listed in Table 1.

Table1: Crystallographic data

	MAC-11	MAC-13	MAC-14
Formula	$C_{24}H_{34}N_6O_{10}Zn_2$	$C_{22}H_{28}N_8O_8Zn_2$	$C_{20}H_{22}N_6O_8Zn_2$
F.W./g·mol^{-1}	697.31	663.26	605.17
Temperature (K)	293(2)	293(2)	293(2)
Wavelength (Å)	0.71073	0.71073	0.71073
Crystal system	Monoclinic	Monoclinic	Monoclinic
Space group	C2/c	C2/c	C2/c
a/Å	39.356(13)	38.503(5)	38.028(10)
b/Å	9.332(3)	9.4511(12)	9.647(3)
c/Å	9.842(3)	9.8023(13)	9.871(3)
β/°	101.864(4)	100.578(2)	97.490(5)
V/$Å^3$	3538(2)	3506.4(8)	3590.3(18)
Z	4	4	4
D_c /g cm^{-3}	1.309	1.241	1.120
μ/mm^{-1}	1.409	1.415	1.375
F(000)	1440	1328	1232
Total collected	8550	10436	12625
Unique data, R(int)	3168, 0.021	3144, 0.059	4053, 0.042
Observed data [I > 2σ(I)]	2811	2249	3017
GOF on F^2	1.10	1.12	1.15
R_1, $wR_2[I > 2\sigma(I)]$	0.0554, 0.1747,	0.0618, 0.2442	0.0845, 0.2759
Peak and hole/e $Å^{-3}$	-0.94, 1.13	-0.84, 1.38	-0.76, 1.36

$R_1 = \Sigma||F_o| - |F_c||/\Sigma|F_o|$. [b] $wR_2 = [\Sigma w(Fo^2 - F_c^2)^2/\Sigma w(F_o^2)^2]^{1/2}$

Synthesis of $\{[Zn_2(dmtrz)_2(L1)]\cdot 6H_2O\}_n$ (MAC-11). $Zn(NO_3)_2\cdot 6H_2O$ (0.3 mmol, 0.089 g) and Hdmtrz (0.2 mmol, 0.018 g) and H_2L1 (0.1 mmol, 0.0271 g) were dissolved in 2 mL DMF. The mixture was stirred at room temperature for 10 min. HNO_3 (0.2 mL) and HBF_4 (0.06 mL) was added to the solution and stirred for another 30 min. The mixture was then transferred into 15 mL Teflon-lined stainless steel vessel, sealed and heated at 140 °C for 3 days under autogenous pressure. Light-yellow sheet crystals of MAC-11 were collected by filtration, washed with acetone for three times, and air-dried (Yield: 62 % based on Zn(II)). Anal. Calcd for $C_{24}H_{34}N_6O_{10}Zn_2$: C, 41.34; H, 4.91; N, 12.05;. Found: C, 41.21; H, 5.08; N, 12.01. FT-IR (KBr pellets, cm^{-1}): 3480(w), 3280(w), 2940(w), 2860(w), 1670(s), 1620(s), 1560(m), 1520(m), 1420(m), 1380(s), 1340(m), 1260(w), 1180(m), 1140 (w), 1090 (m), 1010(w), 856(w), 787(m), 708(w), 650(w).

Synthesis of $\{[Zn_2(dmtrz)_2(L2)]\cdot 4H_2O\}_n$ (MAC-13). The synthesis procedure is analogues to that of MAC-11, except that H_2L1 was replaced by H_2L2. Orange sheet crystals of MAC-13 were isolated in yield of 56% (based on Zn(II)). Anal. Calcd for $C_{22}H_{28}N_8O_8Zn_2$: C, 39.84; H, 4.26; N, 16.89. Found: C, 39.76; H, 4.35; N, 16.81. FT-IR (KBr pellets, cm^{-1}): 3490(m), 2930(w), 2850(w), 1670(s), 1620(s), 1570(w), 1520(w), 1500(w), 1410(m), 1370(s), 1340(w), 1220(w), 1140(w), 1090(w), 1010(w), 877(w), 858(w), 793(m), 708(w), 644(w).

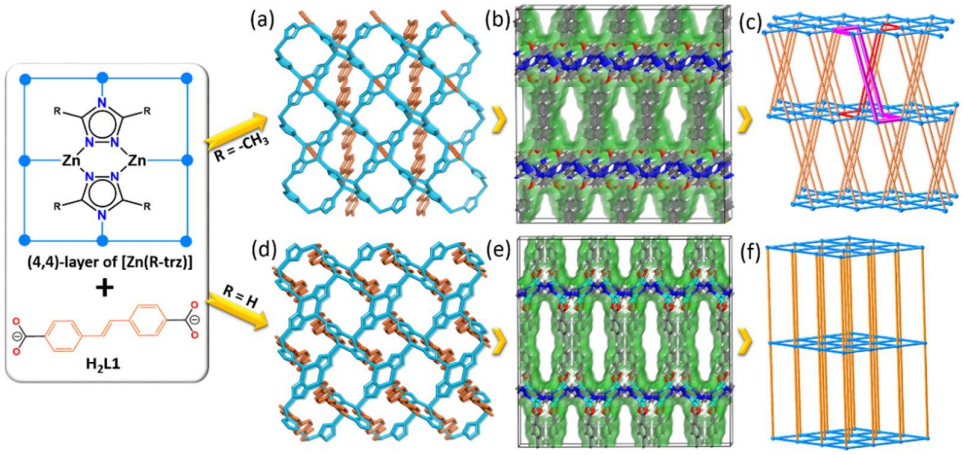

Fig. 1. (a) A top view of MAC-11 showing the arrangement of 2D (4,4)-layers of [Zn(dmtrz)] and stilbenedicarboxylic acid ligands; (b) a side view of MAC-11 showing the 1D channels along *c* axis (Green: Connolly surface with probe atom radii of 1.4 Å, cell: 1 × 4 × 4); (c) the *rob* ($4^8.6^6.8$) net of MAC-11 (the pink and red ring show the self-catenated hopf links); (d) a top view of MAC-14 showing the arrangement of 2D (4,4)-layers of [Zn(trz)] and stilbenedicarboxylic acid ligands; (e) a side view of MAC-14 showing 1D channels along *c* axis; (f) the *pcu* type net of MAC-14.

Synthesis of $\{[Zn_2(trz)_2(L1)]\cdot 4H_2O\}_n$ (MAC-14). The synthesis procedure is analogues to that of MAC-11, except that dmtrz was replaced by trz. Light-yellow sheet crystals of MAC-14 were isolated in yield of 41% (based on Zn(II)). Anal. Calcd for $C_{20}H_{22}N_6O_8Zn_2$: C, 39.69; H, 3.66; N, 13.89. Found: C, 39.61; H, 3.71; N, 13.92. FT-IR (KBr pellets, cm^{-1}): 3447(m), 3126(w), 2931(w), 1670(s), 1606(s), 1550(m), 1522(m), 1386(s), 1299(m), 1215(w), 1166(m), 1092(m), 1038(w), 1007(m), 862(m), 788 (m), 711(w), 667(m).

Results and discussion

Solvothermal reaction of $Zn(NO_3)_2$, Hdmtrz and H_2L1 in DMF solution with additional HNO_3 and HBF_4 leads to the formation of MAC-11. The side product of $[Zn_2(L1)_2H_2O]_n$, which has similar structure as previously reported $[Zn_2(L1)_2(DMF)]_n$,[37, 38] could be obtained without addition acid (Fig. S1 and S2). To isolate pure crystal phase of MAC-11, several acid conditions have been tried, and pure crystal phase without $[Zn_2(L1)_2H_2O]_n$ was finally obtained in the case of HNO_3 (0.2 mL) and HBF_4 (0.06 mL). MAC-11 and MAC-13 are iso-structures (Table 1), only MAC-11 was described here in detail.

Single-crystal diffraction studies revealed that it crystalizes in *C2/c* space group, monoclinic system. Two triazolate ligands coordinate to two Zn ions in $\mu_{1,2}$-bridge mode, generating a $Zn_2(dmtrz)_2$ dimer (Fig. 1, Fig. S3 and Fig. S4 for MAC-13). Then, the dimer unit propagates itself infinitely *via* Zn(1)–N(3) coordinative bond, generating a 2D (4, 4)-connected layer. The average Zn-N bond distance is 2.022 Å, The neighboring 2D layers are further connected together by L1 ligands, resulting into a three-dimensional (3D) lamella structure with 1D channels along *c* axis (Fig. 1b). Considering the $Zn_2(dmtrz)_2$ dimer as a 6-connected node and the L1 ligand as the linear linker, MAC-11 can be considered as a 6-connected framework with a vertex symbol of $4^8.6^6.8$, which is a self-catenated *rob* net with catenated hopf links (Fig. 1d). Similar to that of MAC-11, MAC-14 is also built of two-dimensional Zn-triazolate layers and pillared by L1 ligands (Fig. 1 and Fig. S6). Interestingly, considering the $[Zn_2(trz)_2]$ dimer as a 6-connected node, MAC-14 is a *pcu*-type net rather than a self-catenated *rob* net. Furthermore, their porous structures are confirmed by N_2 sorption isothermal at 77K, giving a BET (Langmuir) surface area of 722 (763), 719 (755) and 677 (831) m^2/g for MAC-11, MAC-13and MAC-14, respectively (Fig. S5a). The pore size is of 5.9, 7.8 and 6.8 Å for MAC-11, MAC-13 and MAC-14 by H-K method [39].

Crystal phase transformation

The PXRD pattern of MAC-11 matches well with the simulated one, confirming the pure crystal phase (Fig.2). It can retain its framework integrity in different solvents, especially in water for at least two days (Fig. S7), confirming its structural stability. We ascribe the robust framework to its unique lamella structure, in which the layer is formed exclusively by strong Zn-N bonds. TGA data (Fig. S8) shows a 15.1 % weight loss from 30 to 150 °C, which could be ascribed to the loss of crystalline water (15.5 wt.%). After that it follows a plateau and then a huge weight loss is observed around 460 °C. Temperature-dependent PXRD revealed a phase transformation from room temperature to 180 °C. The phase transformation occurs in the temperature range of 60 - 90 °C. The diffraction peak at 2θ = 4.6° shifts to 2θ = 5.9° (MAC-11'). According to the index, the peak at 2θ = 4.6° is the reflex of [2 0 0] plane, which belongs to the reflex of the 2D [Zn(dmtrz)] layers. The shortening of the interplanar distance (*d*) from 19.3 Å for MAC-11 to 15.2 Å for MAC-11' suggests a thermo-induced compressed layer structure. Interestingly, MAC-11' can be recovered to its original phase after being soaked in water, demonstrating a reversible phase transformation. Similarly, thermo-induced phase transformation is also observed for MAC-13 (Fig. S9). However, there is no obvious phase transformation for MAC-14 (Fig. S10).

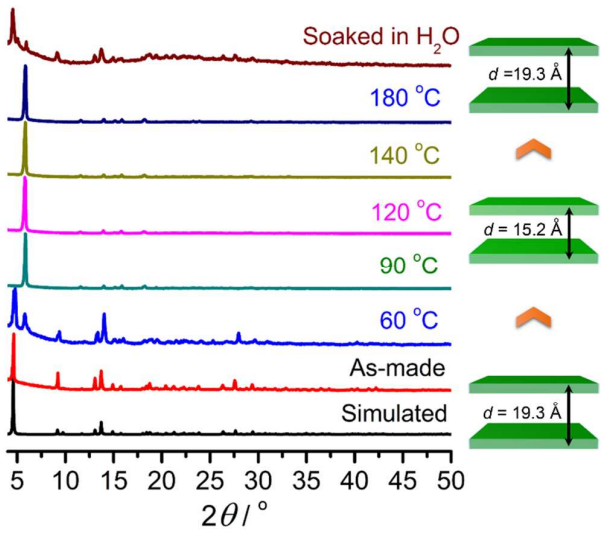

Fig. 2. Reversible crystal phase transformation of **MAC-11**.

The different thermo-induced behaviours may be related to the different connection patterns of pillar ligands to the 2D layers. In MAC-11 and MAC-13, the pillars connect to the neighbouring layers in an offset face-to-face mode and the carboxylate groups coordinate to Zn ions in monodentate fashion. While in MAC-14, the pillars are perpendicular to the layer and carboxylates are hold metal centers in $\eta_{1,2}$-mode.

Photoluminescent response

Upon excitated at λ_{ex} = 369 nm (Fig. 3 and Fig. S11), MAC-11 gives a broad emission with a maximum peak at λ_{em} = 418 nm (two shoulder emissions at 393 and 440 nm). Increasing the temperature to 60 °C, there is no obvious shift but a slight decay in its intensity (Fig.3b). Further increasing the temperature to 90 °C, an obvious shift is observed, which gives a maximum peak at λ_{em} = 453 nm (with two shoulder emissions at 386 and 410 nm). The observable red-shift (35 nm) of the photoluminescent emission indicates a response to the structural transformation. Furthermore, the fluorescent emission can be recovered to its original signal after the phase was recovered. As for MAC-13 (Fig.3c), owing to the strong Uv/Vis absorption of azobenzene, no obvious photoluminescent emission has been detected. As for MAC-14, it has a maximum peak at 442 nm, with two shoulders at 384 and 407 nm. Different from that of MAC-11, no obvious photoluminescent emission shift has been observed for MAC-14 after heating the sample at 90 °C (Fig. S12d).

Mechanism Study

MAC-11 is constructed by 2D layer of photoluminescent [Zn(dmtrz)(COO)] (ligand-to-metal charge transfer, LMCT) pillared by photoluminescent stilbenedicarboxylate (Fig.4). To explore the possible mechanism, the photoluminescent properties of H_2L1 and the 2D layer of $[Zn(dmtrz)(HCOO)]_n$ [40] was studied respectively (Fig.3d, Fig. S12). The emission spectrum of H_2L1 is located in the blue region (440—485 nm) with a maximum peak at 466 nm (a shoulder at 441 nm)

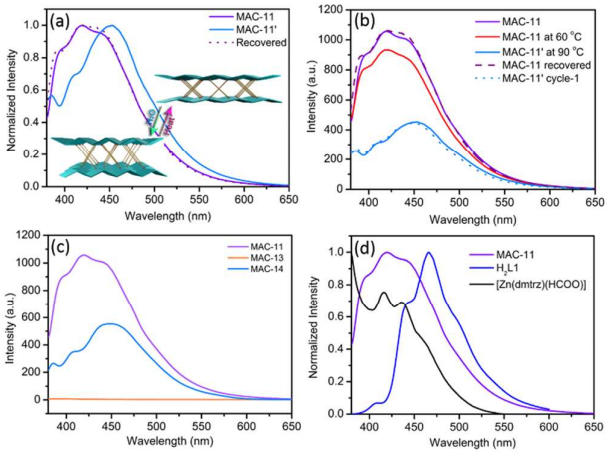

Fig. 3. (a) photoluminescent spectra of MAC-11, MAC-11' and its recovered phase, respectively; (b) the thermo-induced photoluminescent emission transformation of MAC-11; (c) photoluminescent emission of MAC-11, MAC-13 and MAC-14, respectively; (d) photoluminescent secptra of MAC-11 compared with 2D layer of [Zn(dmtrz)(HCOO)] and H_2L1. (Samples are all in solid state and excitated at λ_{ex} = 369 nm)

upon excitated at 369 nm. This emission could be ascribed to the *π-π transition of ligand. For the layer structure of $[Zn(dmtrz)(HCOO)]_n$, the photoluminescent emission is located in the purple region (380—440 nm) with a maximum peak at 416 nm. This emission could be ascribed to the ligand-to-metal charge transition (LMCT). No obvious shift of the photoluminescent emission has been observed for both of them after they were treated at 90 °C for 30 min (Fig. S12a and b). The mechanical mixture of H_2L1 and $[Zn(dmtrz)(HCOO)]_n$ (in a mole ratio of 1 : 2) have also been explored, which gives an emission like H_2L1 with a maximum peak at 464 nm (two shoulders at 408 and 443 nm). No obvious shift of the emission has been detected after the mixture was heated at 90 °C for 30 min (Fig. S12c).

Since there is no obvious photoluminescent shifts for MAC-14, the photoluminescent response to phase transformation of MAC-11 is structural related. Two possible approaches are proposed here: (i) the configurational adjustment of ligands in MAC-11 since it has two different configurations, *trans*- and *cis*-forms; (ii) the rearrangement of the 2D layer of [Zn(dmtrz)] to a more planar one. For the case (i), it is well known that the thermal process can only trigger the transformation of L1 from *cis*- to *trans*-form rather than *trans*- to *cis*-form. Besides, the *trans*-form has a larger π-electron conjugation effect than the *cis*-one, this kind of transformation can only lead to a blue- rather than a red-shift of photolumiescent emission. Therefore, case (i) should be excluded. For the case (ii), the 2D [Zn(dmtrz)] layer is required to be flexible, and then a thermo-induced phase transformation gives a more planar 2D layer. This rearrangement of 2D layer could be accompanied by a slight red-shift of photoluminescent emission owing to an enhanced effect of π-electron conjugation. It has been confirmed that the

Table 2. a short summary of structural parameters with the photoluminescent properties for the related metal-triazolate compounds as well as the structures reported here.

Entry	Compounds	Structure	ω/°	d/Å	ϕ/°	TIPT[a]	λ_{max}/nm	Possible Origin	Ref.
1	$[Zn(dmtrz)Cl]_n$	2D	79.8	2.85	97.4		410	^{1}[LMCT]	42
2	$[Cd(datrz)I]_n$	2D	74.8	2.82	109.7		410	^{1}[LMCT]	42
3	$[Cu(trz)]_n$	2D	0	0	180		468	^{3}[MLCT]	43
4	$[Ag(trz)]_n$	2D	0	0	180		508	^{1}[LMCT]	43
5	$[Zn(dmtrz)(HCOO)]_n$	2D	88.1	2.82	91.6	No	416	^{1}[LMCT]	40
6	MAC-11	3D/*rob*	82.8	2.76	96.1	Yes	418↔453	^{1}[LMCT], ^{1}[π*-π]	this work
7	MAC-13	3D/*rob*	81.9	2.73	97.3	Yes	N.A.	N.A.	this work
8	MAC-14	3D/*pcu*	68.1	2.59	112.4	No	442	^{1}[LMCT], ^{1}[π*-π]	this work
9	H_2L1	0D	N.A.	N.A.	N.A.	No	466	^{1}[π*-π]	this work
10	Mixture of 5 and 9	N.A.	N.A.	N.A.	N.A.	No	466	^{1}[LMCT], ^{1}[π*-π]	this work

[a] TIPT = thermo-induced phase transformation

layered metal-triazolate structure is flexible enough to twist from being markedly corrugated to virtually planar one, [41] and parameters of ω, ϕ, and d are used to assess the state of 2D layer (Fig. 4a,b). The smaller of the parameters are, a more planar 2D layer will be. From Table 2, we can see that the 2D layer [Zn(dmtrz)] in MAC-11 has similar state with that of [Zn(dmtrz)(HCOO)], [Zn(dmtrz)Cl] and [Cd(dmtrz)I]. These compounds have similar emission spectra with peaks around 410 nm. [40] These results suggest that the emission spectra of MAC-11 may originated from the 2D layer of [Zn(dmtrz)]. While, the photoluminescent contribution of pillar L1 ligands could not be excluded because of its slight broadening of the emission spectra. After a thermo-induced phase transformation from MAC-11 to MAC-11', this photoluminescent emission turns quite similar to that of MAC-14. We assume that a thermo-treatment of MAC-11 leads to a decrease of the parameters, resulting a more planar 2D layer of [Zn(dmtrz)]. Therefore, a slight red-shift of the emission spectrum is observed. On the other hand, the vibration band at 1675 cm^{-1} was disappeared from the FT-IR spectra when the phase turns from MAC-11 to MAC-11'. This disappearance indicates an change of the coordinated carboxylate from mono-bridge (μ_1) to chelating ($\eta_{1,2}$) mode (Fig. S13), suggesting an enhanced interaction of L1 ligands to Zn centres. Therefore, the red-shift emission of 2D layer might further be overlaid with that of photoluminescent spectra of stilbenedicarboxylate ligand, giving a maximum emission peak at 453 nm. Taking the structural differences of MAC-11 and MAC-14 in consideration (Fig. 4c,d), the inclination state of the pillared L1 ligands and the flexible 2D layers make it possible for a thermo-induced phase transformation accompanied by photoluminescent response for MAC-11.

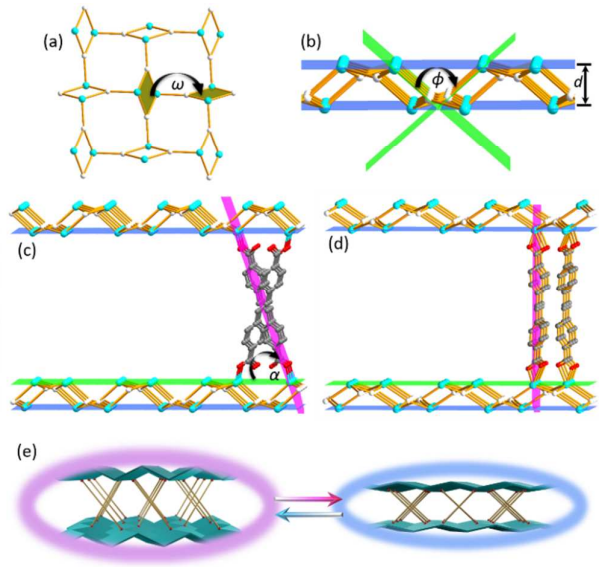

Fig. 4. (a) top view of the simplified 2D metal-triazolate layer showing the ω parameter (green ball: metal center; white ball: the tritopic triazolate); (b) side view of the simplified 2D metal-triazolate layer showing parameters of ϕ, d, respectively; (c) a picture of MAC-11 clearly showing an inclination angle of 70.6° between the 2D layers and the pillar array; (d) a picture of MAC-14 showing a vertical arrangement between them; (e) a view to illustrate the thermo-induced phase transformation accompanied by photoluminescent response.

Conclusions

In this paper, a flexible porous Zinc-coordination polymer of MAC-11 showing a self-catenated *rob*-type net has been successfully synthesized, and an interesting photoluminescent response to a thermo-induced phase transformation has been observed and studied. The robust feature of MAC-11 could be ascribed to its unique layered structure, in which the layer is formed exclusively by Zn-triazolates. Since the π-conjugated triazolate are directly coordinated to metal ions, the thermo-induced phase transformation of 2D Zn-triazolate layer to a more planar one could induce to a sufficient change of the energy state, resulting into a red-shift of the emission spectra. On the other hand, no obvious crystal phase as well as photoluminescent transformation has been observed for the

case of *pcu*-type MAC-14, although it is built of similar photoluminescent modules. So, our studies here not only gives an example of flexible coordination polymer showing thermo/water induced reversible structural-photoluminescent response, but also demonstrates that the framework type also plays an crucial role in affecting the structure-photoluminescent properties.

Acknowledgements

We gratefully acknowledge the financial support from NSFC (Nos. 21201039, 21203032, 21471035), the Shanghai Leading Academic Discipline Project (B108).

Notes and references

§ CCDC number 1063268-1063270 for MAC-11, MAC-13 and MAC-14 respectively.

1 L. Sarkisov, R. L. Martin, M. Haranczyk and B. Smit, *J. Am. Chem. Soc.*, 2014, **136**, 2228-2231.
2 Z. C. Hu, B. J. Deibert and J. Li, *Chem. Soc. Rev.*, 2014, **43**, 5815-5840.
3 S. M. Neville, G. J. Halder, K. W. Chapman, M. B. Duriska, P. D. Southon, J. D. Cashion, J. F. Letard, B. Moubaraki, K. S. Murray and C. J. Kepert, *J. Am. Chem. Soc.*, 2008, **130**, 2869-2876.
4 A. Douvali, A. C. Tsipis, S. V. Eliseeva, S. Petoud, G. S. Papaefstathiou, C. D. Malliakas, I. Papadas, G. S. Armatas, I. Margiolaki, M. G. Kanatzidis, T. Lazarides and M. J. Manos, *Angew. Chem. Int. Ed.*, 2015, **54**, 1651-1656.
5 Y. Yang, P. Du, Y. Y. Liu and J. F. Ma, *Cryst. Growth & Des.*, 2013, **13**, 4781-4795.
6 D. S. Chen, L. B. Sun, Z. Q. Liang, K. Z. Shao, C. G. Wang, Z. M. Su and H. Z. Xing, *Cryst. Growth & Des.*, 2013, **13**, 4092-4099.
7 S. Horike, S. Shimomura and S. Kitagawa, *Nat. chem.*, 2009, **1**, 695-704.
8 L. E. Kreno, K. Leong, O. K. Farha, M. Allendorf, R. P. Van Duyne and J. T. Hupp, *Chem. Rev.*, 2012, **112**, 1105-1125.
9 D. Banerjee, Z. C. Hu and J. Li, *Dalton trans.*, 2014, **43**, 10668-10685.
10 N. Yanai, K. Kitayama, Y. Hijikata, H. Sato, R. Matsuda, Y. Kubota, M. Takata, M. Mizuno, T. Uemura and S. Kitagawa, *Nat. mater.*, 2011, **10**, 787-793.
11 Y. Takashima, V. M. Martinez, S. Furukawa, M. Kondo, S. Shimomura, H. Uehara, M. Nakahama, K. Sugimoto and S. Kitagawa, *Nat. Commun.*, 2011, **2**.
12 S. Y. Liu, X. L. Qi, R. B. Lin, X. N. Cheng, P. Q. Liao, J. P. Zhang and X. M. Chen, *Adv. Funct. Mater.*, 2014, **24**, 5866-5872.
13 H. J. Choi, M. Dinca and J. R. Long, *J. Am. Chem. Soc.*, 2008, **130**, 7848-7849.
14 D. N. Dybtsev, H. Chun and K. Kim, *Angew. Chem. Int. Ed.*, 2004, **43**, 5033-5036.
15 B. L. Chen, C. D. Liang, J. Yang, D. S. Contreras, Y. L. Clancy, E. B. Lobkovsky, O. M. Yaghi and S. Dai, *Angew. Chem. Int. Ed.*, 2006, **45**, 1390-1393.
16 F. X. Coudert, A. Boutin, M. Jeffroy, C. Mellot-Draznieks and A. H. Fuchs, *Chemphyschem*, 2011, **12**, 247-258.
17 S. Bourrelly, P. L. Llewellyn, C. Serre, F. Millange, T. Loiseau and G. Ferey, *J. Am. Chem. Soc.*, 2005, **127**, 13519-13521.
18 A. Kondo, H. Noguchi, S. Ohnishi, H. Kajiro, A. Tohdoh, Y. Hattori, W. C. Xu, H. Tanaka, H. Kanoh and K. Kaneko, *Nano. Lett.*, 2006, **6**, 2581-2584.
19 S. Henke, W. Li and A. K. Cheetham, *Chem Sci*, 2014, **5**, 2392-2397.
20 J. J. Low, A. I. Benin, P. Jakubczak, J. F. Abrahamian, S. A. Faheem and R. R. Willis, *J. Am. Chem. Soc.*, 2009, **131**, 15834-15842.
21 D. K. Maity, B. Bhattacharya, R. Mondal and D. Ghoshal, *CrystEngComm*, 2014, **16**, 8896-8909.
22 Z. Xue, T. Sheng, Y. Wang, S. Hu, Y. Wen, Y. Wang, H. Li, R. Fu and X. Wu, *CrystEngComm*, 2015, **17**, 2004-2012.
23 G. Ferey and C. Serre, *Chem. Soc. Rev.*, 2009, **38**, 1380-1399.
24 J. P. Zhang, Y. B. Zhang, J. B. Lin and X. M. Chen, *Chem. Rev.*, 2012, **112**, 1001-1033.
25 T. M. McDonald, Z. R. Herm, E. D. Bloch, K. Sumida, J. A. Mason and J. R. Long, *Abstr Pap Am Chem S*, 2012, **243**.
26 H. Hayashi, A. P. Cote, H. Furukawa, M. O'Keeffe and O. M. Yaghi, *Nat. mater.*, 2007, **6**, 501-506.
27 L. Hou, Y. Y. Lin and X. M. Chen, *Inorg. Chem.,* 2008, **47**, 1346-1351.
28 R.B. Lin, F. Li, S.-Y. Liu, X.L. Qi, J.P. Zhang, and X.M. Chen, Angew. Chem. Int. Ed. 2013, **52**, 13429-13433.
29 B. B. Tu, Q. Q. Pang, D. F. Wu, Y. N. Song, L. H. Weng and Q. W. Li, *J. Am. Chem. Soc.*, 2014, **136**, 14465-14471.
30 B. Xia, Z. X. Chen, Q. S. Zheng, H. Zheng, M. L. Deng, Y. Ling, L. H. Weng and Y. M. Zhou, *CrystEngComm.*, 2013, **15**, 3484-3489.
31 F. L. Yang, Q. S. Zheng, Z. X. Chen, Y. Ling, X. F. Liu, L. H. Weng and Y. M. Zhou, *CrystEngComm.*, 2013, **15**, 7031-7037.
32 Q. S. Zheng, F. L. Yang, M. L. Deng, Y. Ling, X. F. Liu, Z. X. Chen, Y. H. Wang, L. H. Weng and Y. M. Zhou, *Inorg. Chem.*, 2013, **52**, 10368-10374.
33 I. T. MacLeod, E. R. T. Tiekink and C. G. Young, *J. Organomet. Chem.*, 1996, **506**, 301-306.
34 X. S. Wang, S. Q. Ma, K. Rauch, J. M. Simmons, D. Q. Yuan, X. P. Wang, T. Yildirim, W. C. Cole, J. J. Lopez, A. de Meijere and H. C. Zhou, *Chem. Mater.*, 2008, **20**, 3145-3152.
35 G. M. Sheldrick, SHELXL-2013, Program Crystal Structure Refinement, University of Göttingen, Germany, 2013.
36 G. M. Sheldrick, SHELXS-2013, Programs for X-ray Crystal Structure Solution, University of Göttingen, Germany, 2013.
37 C.A. Bauer, T. V. Timofeeva, T. B. Settersten, B. D. Patterson, V. H. Liu, B. A. Simmons, and M. D. Allendorf, J. Am. Chem. Soc., 2007, 129, 7136-7144.
38 H. Kim, G. Park and K. Kim, *CrystEngComm*, 2008,10, 954-956.
39 G. Horvath and K. Kawazoe, *J. Chem. Eng. Jpn.* 1983, 16, 470-475.
40 A. X. Zhu, J. B. Lin, J. P. Zhang and X. M. Chen, *Inorg. Chem.*, 2009, **48**, 3882-3889.
41 Y. Y. Lin, Y. B. Zhang, J. P. Zhang and X. M. Chen, *Cryst. Growth & Des.*, 2008, **8**, 3673-3679.
42 Q. G. Zhai, X. Y. Wu, S. M. Chen, C. Z. Lu and W. B. Yang, *Cryst. Growth & Des.*, 2006, **6**, 2126-2135.
43 J. P. Zhang, Y. Y. Lin, X. C. Huang and X. M. Chen, *J. Am. Chem. Soc.*, 2005, **127**, 5495-5506.

A self-catenated *rob*-type porous coordination polymer constructed from triazolate and carboxylate ligands: fluorescent response to the reversible phase transformation

Mingli Deng, Shijun Tai, Weiquan Zhang, Yongchen Wang, Jiaxing Zhu, Jinsheng Zhang, Yun Ling* and Yaming Zhou

A flexible porous Zinc-coordination polymer of **MAC-11** showing self-catenated *rob*-type net has been successfully synthesized, and an interesting photoluminescent response to a thermo-induced phase transformation has been observed and studied.